**USING SIMULATED MICROMETEOROID IMPACTS TO UNDERSTAND THE PROGRESSIVE SPACE WEATHERING OF THE SURFACE OF MERCURY.** M. S. Thompson[1], M. L. McGlaun[1], K. E. Vander Kaaden[2], M. J. Loeffler[3], and F. M. McCubbin[4]. [1]Department of Earth, Atmospheric, and Planetary Sciences, Purdue University, West Lafayette, IN, 47907, (mthompson@purdue.edu) [2]Jacobs, NASA Johnson Space Center, Houston, TX, 77058, [3]Northern Arizona University, Flagstaff, AZ, 86011, [4]ARES, NASA Johnson Space Center, Houston, TX, 77058.

**Introduction:** The surfaces of airless bodies such as Mercury are continually modified by space weathering, which is driven by micrometeoroid impacts and solar wind irradiation [1,2]. Space weathering alters the chemical composition, microstructure, and spectral properties of surface regolith. In lunar and ordinary-chondritic style space weathering, these processes affect the reflectance properties by darkening (lowering of reflectance), reddening (increasing reflectance with increasing wavelength), and attenuation of characteristic absorption features [2]. These optical changes are driven by the production of nanophase Fe-bearing particles (npFe). While our understanding of these alteration processes has largely been based on data from the Moon and near-Earth S-type asteroids, the space weathering environment at Mercury is much more extreme [3]. The surface of Mercury experiences a more intense solar wind flux and higher velocity micrometeoroid impacts than its planetary counterparts at 1 AU [4]. Additionally, the composition of Mercury's surface varies significantly from that of the Moon. Most notably, a very low albedo unit has been identified on Mercury's surface, known as the low reflectance material (LRM). This unit is enriched with up to 4 wt.% carbon, likely in the form of graphite, over the local mean [5]. In addition, the surface concentration of Fe across Mercury's surface is low (<2 wt.%) compared to the Moon [6]. Our understanding of how these low-Fe and carbon phases are altered as a result of space weathering processes is limited. Since Fe plays a critical role in the development of space weathering features on other airless surfaces (e.g., npFe), its limited availability on Mercury may strongly affect the space weathering features in surface materials.

In order to understand how space weathering affects the chemical, microstructural, and optical properties of the surface of Mercury, we can simulate these processes in the laboratory [7]. Here we used pulsed laser irradiation to simulate the short duration, high-temperature events associated with micrometeoroid impacts. We used forsteritic olivine, likely present on the Mercurian surface, with varying FeO contents, each mixed with graphite, in our experiments. We then performed reflectance spectroscopy and electron microscopy to investigate the spectral, chemical, and microstructural changes in these samples.

**Methods:** Starting silicate compositions consisted of a series of forsteritic olivines with varying FeO contents synthesized at 1-bar at NASA's Johnson Space Center [8]. Using these samples, we prepared three pressed powder pellets for laser irradiation, each with a base layer of olivine (to maintain pellet structure) and a surface layer containing the graphite-olivine mixture: 1) Sample SC-001 with San Carlos olivine (Fo90.91) mixed with 5 wt.% powdered graphite, 2) Sample F-S-002 with 0.05 wt.% FeO olivine mixed with 5 wt.% graphite, and 3) F-T-004 with 0.53 wt.% FeO olivine mixed with 5 wt.% graphite [8]. The grain sizes for each sample ranged from 45 to 125 μm. Samples were irradiated at Northern Arizona University using a pulsed Nd-YAG laser, ($\lambda$=1064 nm, ~6 ns pulse duration, energy of 48 mJ/pulse) while under vacuum. For each sample the laser was rastered 1x and then 5x over the surface. We collected *in situ* reflectance spectra from the surfaces of the samples after each individual laser pulse using a Nicolet IS50 Fourier-Transform Infrared spectrometer (wavelength range of 0.65-2.5 μm). We used an FEI Nova NanoSEM200 scanning electron microscope (SEM) at Purdue University to image the surface morphology and topography of the samples. We used an FEI Helios NanoLab 660 focused ion beam (FIB) SEM at the University of Arizona to extract thin sections for future analysis in the transmission electron microscope (TEM).

**Reflectance Spectroscopy Results:** Reflectance spectra for each sample are shown in Fig. 1.

*SC-001:* The spectrum of the unirradiated sample exhibits low reflectance and a weak 1.0 μm absorption feature, associated with $Fe^{2+}$ in the olivine (Fig. 1a). After 1x laser shot, the reflectance of this sample is higher, and the absorption feature increases in strength. After 5x laser shots the sample reflectance is the lowest of any sample evaluated and the 1.0 μm absorption feature is weakest.

*F-T-004:* The unirradiated sample has a blue-sloped spectrum with low reflectance and no visible absorption features (Fig. 1b). With progressive laser irradiation, the reflectance of the sample increases and becomes strongly red-sloped in the 5x lasered sample.

*F-S-002:* The unirradiated samples exhibit the darkest spectrum and is blue-sloped. After experiencing laser irradiation, the brightness of this sample increases dramatically from ~0.18 average reflectance in the unirradiated sample to over 0.8 reflectance in the 5x irradiated sample (Fig. 1c). The slope of the spectra for the laser irradiated samples are slightly reddened compared to the unirradiated sample.

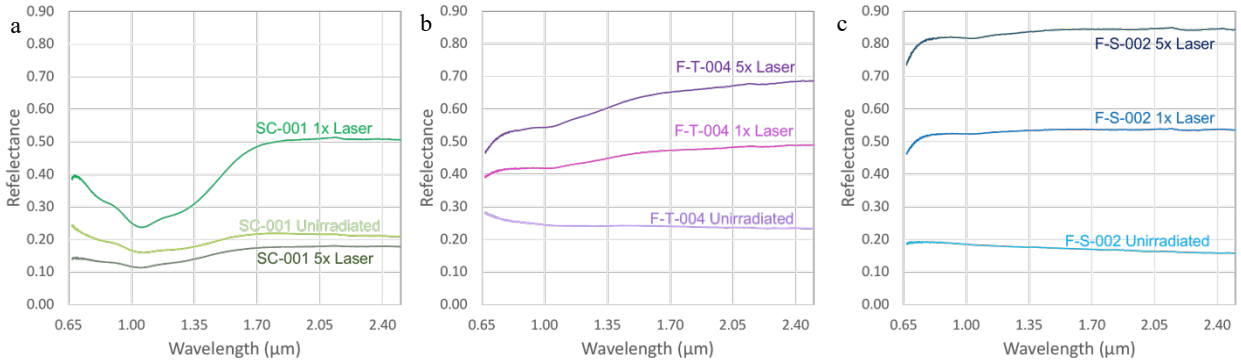


**Figure 1:** Reflectance data for the a) San Carlos olivine, b) F-T-004, and c) F-S-002 samples showing spectra for unirradiated material, after 1x laser shot, and after 5x laser shots. All spectra are presented on same reflectance scale.

**Morphological and Microstructural Analysis:** There are two alteration textures observed in the samples exposed to simulated space weathering: 1) fluffy C-rich, and 2) vesiculated melt. The fluffy C-rich texture is evident in the 5x laser shot samples (Fig. 2a) and is composed of fine-grained, apparent low-density deposits of C-rich material across the surface. These textures may correspond to the C 'globules' observed previously in SC-001 [9]. This microstructure is considerably different from the graphite we observe at depth in the sample, comprised of discretely stacked layers, which appears unaltered by the laser. The second texture is a smooth and uniform melt layer distributed across isolated regions of the sample surface which contains vesicles ranging up to 100s of nm in diameter (Fig. 2b). FIB sections have been extracted from each of these textures for each sample to examine in detail their microstructural and chemical characteristics.

**Implications for Space Weathering on Mercury:** Previous experiments simulating space weathering of Mercury have shown darkening and reddening of spectra [7,10]. In contrast, here we observe brightening with progressive irradiation in the F-S-002 and F-T-004 samples. These changes may be due to the graphite-bearing overlayer beginning to disintegrate during irradiation, revealing underlying bright material. However, it is possible that the amalgamation of small graphite particles into the fluffy C-rich textures observed on the surface may also contribute to this spectral change. The inclusion of low-Fe minerals *and* C-bearing phases in these experiments are more analogous to the Mercurian surface than previous work and our results indicate that sample composition plays a significant role in space weathering on Mercury. There is a strong correlation of spectral slope with Fe content after irradiation. Variation between the F-S-002 and F-T-004 samples is <0.6 wt.% and yet the spectra deviate from flat to strongly reddened. We will explore the microstructural and chemical causes for these variations through TEM analysis.

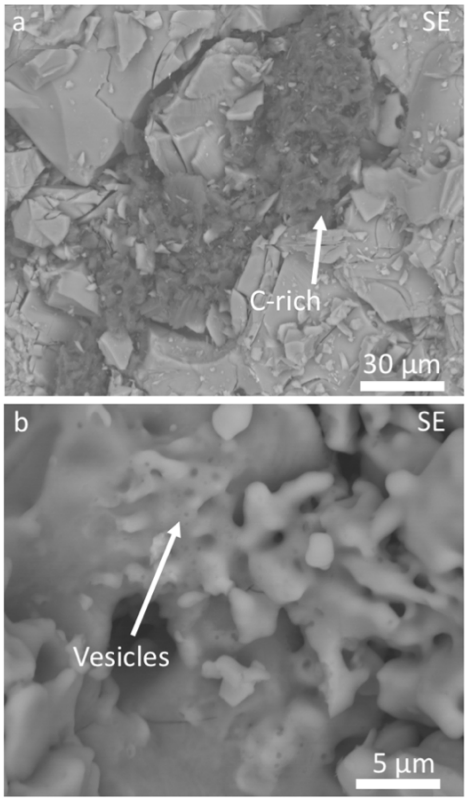


**Figure 2:** Secondary electron (SE) images of the surface morphology of the a) F-S-002 sample showing fluffy C-rich textures, and the b) F-T-004 sample showing the vesiculated melt texture.

**References:** [1] Hapke B. (2001) *J. Geophys. Res.-Planet., 106,* 10039–10073. [2] Pieters C.M. and Noble S.K. (2016) *J. Geophys. Res-Planet., 121,* 1865–1884. [3] Lucey P.G., and Riner, M.A. (2011) *Icarus,* 212, 451-462. [4] Cintala M.J. (1992) *J. Geophys. Res.-Planet., 97,* 947–973. [5] Klima R.L. et al. (2018) *Geophys. Res. Letters*, *45*, 2945–2953. [6] Nittler L.R., et al. (2011) *Science 333,* 1847-1850. [7] Sasaki S. and Kurahashi E. (2004) Space weathering on Mercury, *Adv. Space Res.*, 33, 2152-2155. [8] Vander Kaaden K.E., et al. (2018) *LPSC XLIX,* Abstract 1230. [9] McGlaun M.L. et al. (2019) *LPSC L,* Abstract 2019. [10] Trang D. et al. (2018) *LPSC XLIX,* Abstract 2083.